Experimental clathrate superhydrides EuH_6 and EuH_9 at extreme pressure conditions

Liang Ma,[1,2,3,*] Mi Zhou,[2,*] Yingying Wang,[1,2] Saori Kawaguchi,[4] Yasuo Ohishi,[4] Feng Peng,[5] Hanyu Liu,[2] Guangtao Liu,[2,†] Hongbo Wang,[1,2,‡] and Yanming Ma[1,2,3,§]

[1]*State Key Laboratory of Superhard Materials, College of Physics, Jilin University, Changchun 130012, China*
[2]*International Center of Computational Method & Software, College of Physics, Jilin University, Changchun 130012, China*
[3]*International Center of Future Science, Jilin University, Changchun 130012, China*
[4]*Japan Synchrotron Radiation Research Institute, Sayo, Hyogo 679-5198, Japan*
[5]*College of Physics and Electronic Information, Luoyang Normal University, Luoyang 471022, China*

(Received 26 July 2020; accepted 26 October 2021; published 12 November 2021)

The recent discovery of a class of sodalitelike clathrate superhydrides (e.g., YH_6, YH_9, ThH_9, ThH_{10}, and LaH_{10}) at extreme pressures, which commonly exhibit high-temperature superconductivity with the highest T_c approaching 260 K for LaH_{10}, opened up a new era in the search for high-temperature superconductors in metal superhydrides. There is high interest in finding alternative clathrate superhydrides that might witness the long-dreamed room-temperature superconductivity. Here, we target the experimental synthesis of europium (Eu) superhydrides where theory can fail for the prediction of superconductivity. We pressurized and laser heated a mixture of metal Eu and ammonia borane (NH_3BH_3) in a diamond-anvil cell and successfully synthesized the clathrate structured EuH_6 and EuH_9 at conditions of 152 GPa and 1700 K, and 170 GPa and 2800 K, respectively. Two nonclathrate structured phases of EuH_5 and EuH_6 were also synthesized that are not reported in lanthanide superhydrides. Theoretical simulations predicted that all the synthesized europium hydrides are magnetic, where the electrical resistance measurements suggest a possible magnetic order transition temperature at around 225 and 258 K, respectively, for EuH_5 and clathrate EuH_6. Our work has created a model superhydride platform for subsequent investigations on how a strongly correlated effect and magnetism can affect the superconductivity of superhydrides.

DOI: 10.1103/PhysRevResearch.3.043107

I. INTRODUCTION

The quest for atomic metallic hydrogen (AMH) has proven extremely challenging due to the requirements of ultrahigh-pressure conditions and supersensitive characterizations [1–4]. Alternatively, in 2012, there was a theoretical proposal on potential high T_c superconductivity in superhydride CaH_6 (a theoretical $T_c = 235$ K at 150 GPa) stabilized at high pressures [5]. The key to the unusually high T_c superconductivity lies in the formation of a Ca-doped AMH within a peculiar H clathrate structure containing enclathrated Ca in a crystal lattice, giving rise to a large H-derived electronic density of states (DOS) at the Fermi level and extremely strong electron-phonon coupling related to H-H vibrations in the H cages [5]. The formation of a clathrate structure in group IV elements is common since the elements' four valence electrons are ready to accept four covalent bonds to stabilize the clathrate cage [6,7]. However, such a clathrate structure for hydrogen that contains only one valence electron is quite unusual, and becomes possible only when hydrogen accepts a sufficient number of extra electrons from Ca atoms under high-pressure conditions [5].

Following the first prediction of CaH_6, the same clathrate structure was later proposed in YH_6 and MgH_6 with a predicted $T_c = 264$ K at 120 GPa [8] and $T_c = 260$ K at 300 GPa [9], respectively. These two latter superhydrides together with CaH_6 share a common feature of high-temperature superconductivity with theoretical T_c values all exceeding 200 K. This appearance inevitably generated a great deal of attention towards finding of high T_c superconductors in clathrate superhydrides [10,11].

In 2017, along the line of finding clathrate structures in superhydrides, major theoretical progress was achieved via a comprehensive crystal structure searching simulation on rare-earth (RE) superhydrides at high pressures [10]. The results elucidated that the pressure-induced formation of clathrate structures is a general behavior for all RE superhydrides. Besides REH_6 that shares the same clathrate structure with that of CaH_6, two other unexpected clathrate stoichiometries of REH_9 and REH_{10} having a higher H content than that of CaH_6 were also reported. Though all of them are clathrate structures, different H_{24}, H_{29}, and H_{32} cages for stoichiometries REH_6, REH_9 and REH_{10}, respectively, emerged, which could be accepted as a critical role in improving the superconductivity in these superhydrides. Notably, high-temperature superconductivity appears frequently in these RE superhydrides with

*These authors contributed equally to this work.
†liuguangtao@jlu.edu.cn
‡whb2477@jlu.edu.cn
§mym@jlu.edu.cn

the predicted $T_c = 276$ K at 150 GPa for YH_9, $T_c = 303$ K at 400 GPa for YH_{10}, and $T_c = 288$ K at 200 GPa for LaH_{10} [10]. It should be particularly emphasized that the predicted clathrate structure and high-temperature superconductivity of LaH_{10} and YH_{10} in our work of Ref. [10] coincide exactly with the results from another independent theoretical work [11] appearing at nearly the same time.

With the guidance of the theoretical prediction in Refs. [10,11], experimental progress on the synthesis of these clathrate superhydrides has been remarkable [12–27]. A major move was made on the observation of near-room-temperature superconductivity in the clathrate LaH_{10} with T_c approaching 260 K [12,13]. Subsequent syntheses of other clathrate superhydrides of YH_6 [19,21], YH_9 [20,21], ThH_9, ThH_{10} [16], CeH_9, CeH_{10} [26], $(LaY)H_6$, $(LaY)H_{10}$ [22], and probable CaH_6 [24,25] with observed high T_c values in the range of 146–253 K added more examples to the family of clathrate superhydrides, a new class of high-temperature superconductors holding a highest T_c value of 260 K. The clathrate superhydrides PrH_9 and NdH_9 that were first predicted in Ref. [10] were also experimentally synthesized [18,27], but the superconducting transition temperatures were measured to be below 10 K, where the superconductivity is apparently suppressed by the emergence of magnetic ordering as suggested. These results indicate, beside hydrogen clathrate cages, other physical properties are also important for affecting the superconductivity of superhydrides, e.g., magnetism and strongly correlated effects. Solving this issue requires advances in exploring the stable structures and fundamental physics properties (magnetism, strongly correlated effects, superconductivity, etc.) of clathrate superhydrides.

Eu, one of the most reactive rare-earth elements and an electronically strongly correlated metal [28,29], adopts a divalent state at an ambient condition with a strong local magnetic moment [30]. At high pressure, magnetic order in Eu is observed to collapse just above 80 GPa as superconductivity emerges, even though there are strong local $4f^7$ magnetic moments at higher pressure [30–33]. In the H-rich conditions, Eu can accept hydrogen to form dihydrides or even trihydrides below 10 GPa [34,35]. Our previous simulations [10] predicted that Eu can react with hydrogen to form the clathrate superhydrides EuH_6, EuH_9, and EuH_{10} at high pressures.

In this paper, we target the synthesis of Eu superhydrides under high-pressure conditions using a laser-heated diamond-anvil cell technique via a mixture of Eu and ammonia borane with the aim of finding clathrate superhydrides, allowing us to subsequently investigate how magnetism and a strongly correlated effect in the electronic structure can affect the superconductivity of superhydrides. Encouragingly, we did synthesize a series of Eu superhydrides of EuH_3, EuH_5, EuH_6, and EuH_9 in the pressure range of 80–170 GPa. All the synthesized europium hydrides are found to be magnetic through our theoretical calculations.

II. METHODS

The experiments in the present work were conducted using laser-heated diamond-anvil cell (DAC) techniques. The diamonds used in DACs had a culet with a diameter of 60–80 μm and were beveled at 8° to a diameter of about 280 μm. Europium hydrides were synthesized via a reaction of Eu (Alfa Aesar 99.99% purity) and BH_3NH_3 (Sigma-Aldrich 97% purity) at high-pressure and high-temperature conditions. The use of BH_3NH_3 as a source of H_2 has been demonstrated to be reliable by previous excellent results [12,17,19]. Composite gaskets consisting of a rhenium outer annulus and a mixture of cubic boron nitride (c-BN) and an epoxy (Embed-It^{TM} Low Viscosity Epoxy Kit) insert was employed to contain the sample while isolating the electrical leads in the electrical measurements. The temperature dependence of resistance was measured via the four-probe van der Pauw method with four Pt electrodes. Sample preparation and initial loading of the anvils were done in an inert Ar atmosphere (less than 0.01 ppm of oxygen and water) in a glove box to guarantee that the sample was properly isolated from the surrounding atmosphere. Afterwards, the sample was compressed to the target pressure at room temperature. The pressures in all the experiments were determined from the shift in the high-frequency edge of the Raman spectrum gathered from the stressed tip of the diamond anvil at room temperature [36]. In our experience, we found that the pressure increases slightly by about 5 GPa during the cooling process.

In situ x-ray diffraction (XRD) data presented in this work were collected at the BL10XU beamline at the SPring-8 facility (Hyogo, Japan) [37] with a wavelength of 0.4136 Å, and the x-ray spot size was around 3 μm × 2 μm. An imaging plate detector (RAXIS-IV; Rigaku) was used to collect the angle-dispersive XRD data. Primary processing and integration of the powder patterns were carried out using the DIOPTAS software [38]. Parts of the preliminary XRD measurements were also performed at the Shanghai Synchrotron Radiation Facility Beamline BL15U1 and Beijing Synchrotron Radiation Facility HP-Station 4W2. The Rietveld refinements were done using GSAS and EXPGUI packages [39]. The laser-heating experiments were performed by a two-sided SPI fiber laser with 1050 nm at BL10XU in SPring-8, and the temperature was determined by fitting the emission spectra from the surface of the heated sample to Planck's radiation law. All the crystal structure information obtained in this work is summarized in Table S1 [40].

The equations of state (EOS) of EuH_2, EuH_3, EuH_6, and EuH_9 phases were calculated using density functional theory (DFT) [41,42] within the generalized gradient approximation (Perdew-Burke-Ernzerhof functional) [43], and the projector augmented-wave method [44,45] as implemented in the VASP code [46–48]. The electron-ion interaction was described with the $5s^26s^25p^64f^7$ and $1s^1$ configurations treated as valence electrons for Eu and H, respectively. To ensure that all enthalpy calculations were well converged to about 1 meV/atom, the Brillouin zone was sampled using Γ-centered k-point meshes with a sufficient density ($2\pi \times 0.03$ Å^{-1}) in reciprocal space, as well as a kinetic energy cutoff of 800 eV. Eu has a half-filled f shell, therefore the on-site Coulomb interactions are described by using the DFT+U method with $U = 7.0$ eV [49]. The dependences of the volume on pressure were fitted by the third-order Birch-Murnaghan equation [50] to determine the main parameters of the EOS.

III. RESULTS AND DISCUSSION

In our earlier theoretical study [10], a convex hull of Eu hydrides was constructed through density functional total-energy calculations to find that EuH_4 and clathrate EuH_9 are stable compounds, while clathrate EuH_6 and EuH_{10} lie above the convex hull in the whole pressure range of 100–400 GPa. Motivated by the theoretical results, we prepared four DACs referred to as samples C1, C2, C3, and C4, where a 2-μm-thick sample of Eu was sandwiched between two BH_3NH_3 layers in a c-BN sample chamber. All samples are pressurized to 80–170 GPa in order to synthesize the clathrate superhydrides.

In sample C1, the pressure was loaded to 80 GPa at room temperature and then heated to 1400 K by a laser. The measured XRD pattern was plotted in Fig. 1(a). We found that the resultant products were dominated by an fcc lattice, which could be identified as EuH_2 or EuH_3. However, it is difficult to distinguish them based on the current experimental data since their difference in lattice volume is too small. We then performed the enthalpy calculation and found that EuH_3 has a much lower enthalpy of 0.557 eV/atom than that of $EuH_2 + \frac{1}{2}H_2$ when H_2 is in an excessive environment. From such an energy consideration, the fcc phase was thus identified as EuH_3. It is noteworthy that EuH_3 with a cubic close packing of Eu atoms is isostructural to the ambient structure of LaH_3 [51], where each Eu atom is coordinated by eight H atoms [Fig. 1(b)]. The shortest H-H distance is 2.01 Å at 80 GPa.

After the first heating, the sample was further compressed to 130 GPa and then heated to ~1600 K. The integrated XRD pattern is shown in Fig. 1(c). A new phase was evident and considered to be a cubic lattice which is similar to the structure of β-UH_3 [52]. But from an EOS comparison, we found the experimental volume of the new phase is much larger than the calculated volume of the EuH_3 structure (Fig. S1 [40]), therefore, we considered the presence of additional hydrogen in the same metal sublattice with that of β-UH_3. Structure searches of stoichiometric EuH_4, EuH_5, and EuH_6 at 150 GPa with a fixed position of Eu atoms were performed using the swarm-intelligence-based CALYPSO structure prediction method [53,54]. We predicted a metastable $Pm\bar{3}n$ structure of EuH_5 [Fig. 1(d)], the EOS of which is consistent with experimental P-V data (Fig. S1 [40]). This structure contains two inequivalent positions of Eu: One Eu atom in position I is surrounded by 12 H atoms at the corners of an icosahedron and another Eu atom in position II is surrounded by six H atoms forming a hexahedron. H_2 quasimolecules are evenly distributed in the interspace of icosahedrons.

In sample C2, the initial pressure was loaded up to 92 GPa and heated to a temperature of 3100 K. The XRD patterns [Fig. 1(e)] obtained indicate an unexpected hexagonal structure of EuH_6 which is a nonclathrate structure and was first theoretically reported in ScH_6 [55], consisting of H-sharing 12-fold EuH_{12} octahedrons [Fig. 1(f)]. In this structure, hydrogen takes a quasimolecular state with d(H-H) = 1.143 Å.

In order to synthesize the targeted clathrate structures, sample C3 was directly compressed to an ultrahigh pressure of 152 GPa and laser heated to a temperature of 1700 K. The measured XRD patterns of the sample [Fig. 2(a)] match the sodalitelike clathrate EuH_6 predicted in Ref. [10]. In the

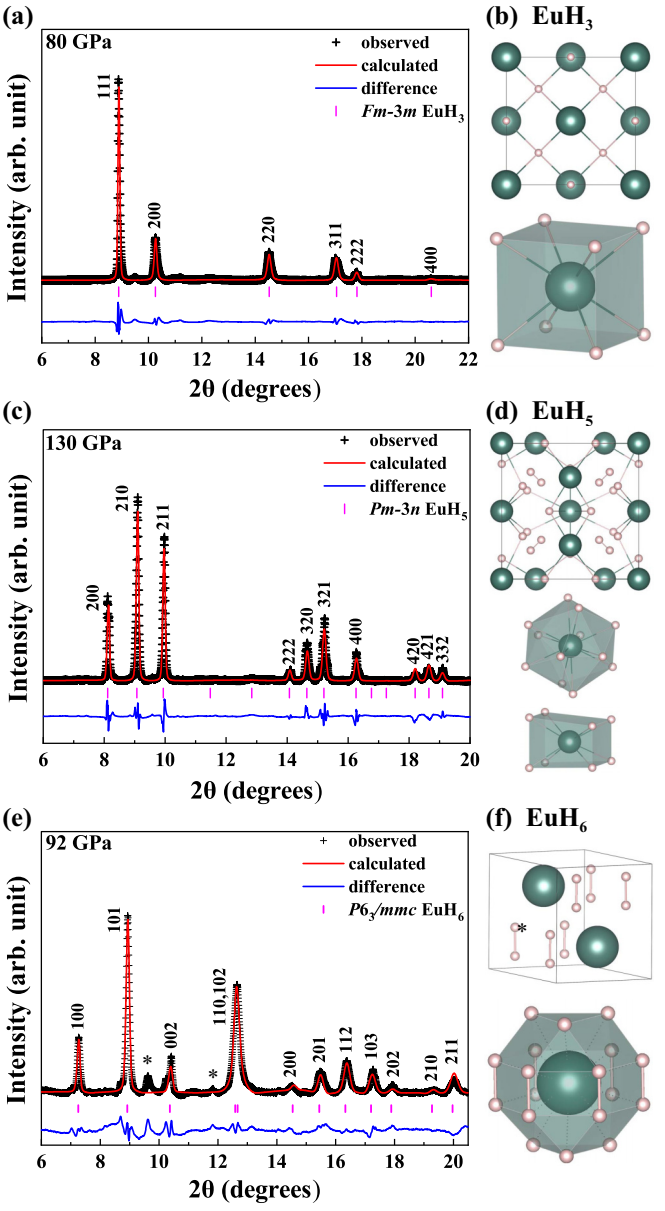

FIG. 1. Rietveld refinement of the experimental XRD pattern (left panel) and crystal structures (right panel) of (a), (b) EuH_3 at 80 GPa, (c), (d) EuH_5 at 130 GPa, and (e), (f) nonclathrate EuH_6 at 92 GPa. Large and small balls represent the Eu atoms and H atoms, respectively.

structure, each Eu atom is surrounded by 24 H atoms forming a H_{24} cage and each cage is composed of six squares and eight hexagons [Fig. 2(b)]. The H-H distance is 1.3 Å and the nearest Eu-H distance is 2.051 Å at 152 GPa. This structure was first predicted in CaH_6 [5], but first synthesized in YH_6 [19,21]. EuH_6 is the second synthesized example and the first hexahydride synthesized in lanthanide hydrides. During the release of pressure, the clathrate EuH_6 can be stabilized to at least 87 GPa, at a lower pressure which gradually decomposes into the EuH_5 phase and H_2 [Fig. 3(a)].

Sample C4 was heated to 2800 K with a loaded pressure at 170 GPa, aiming to synthesize superhydrides with a higher hydrogen content. The analysis of the measured XRD patterns

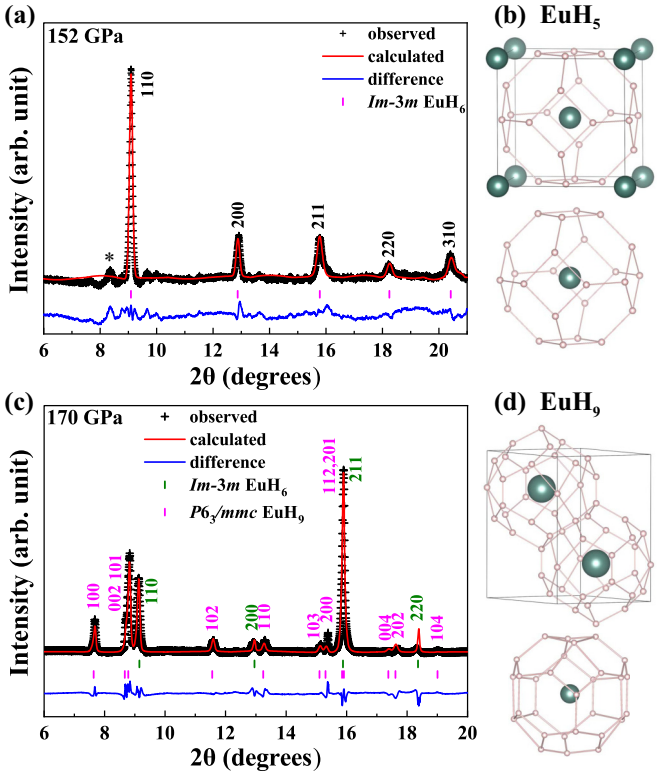

FIG. 2. Rietveld refinement of the experimental XRD pattern (left panel) and crystal structures (right panel) of (a), (b) clathrate EuH_6 at 152 GPa, and (c), (d) the mixture of clathrate EuH_6 and EuH_9 at 170 GPa. Large and small balls represent the Eu atoms and H atoms, respectively.

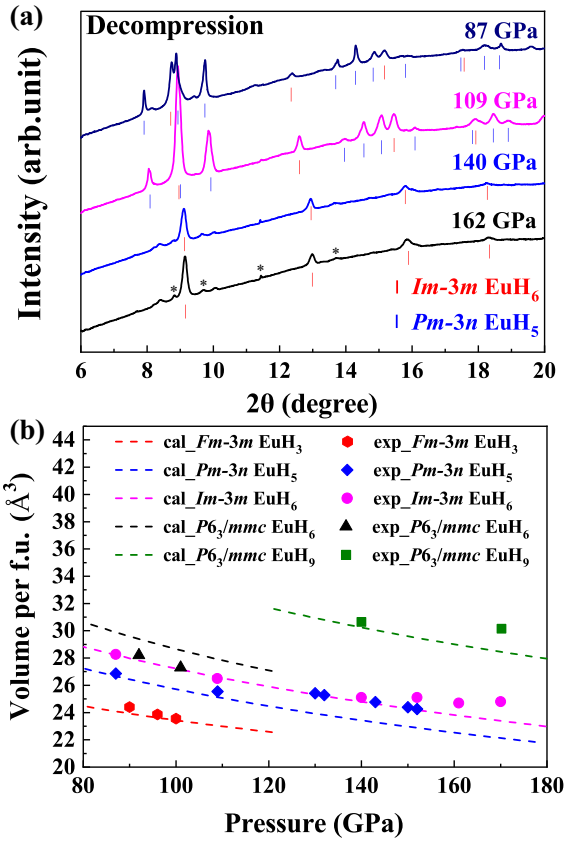

FIG. 3. (a) Experimental XRD patterns during decompression of sample C3 in the pressure range of 162–87 GPa. (b) The comparison of fitting EOS of all stoichiometries with the experimental *P-V* data. The dashed curves represent the calculated EOS. The symbols represent the experimental result.

showed that besides EuH_6, the clathrate stoichiometry EuH_9 predicted in our previous work [10] was successfully synthesized [Fig. 2(c)] at this condition. The weight fractions of the EuH_6 and EuH_9 phases in the mixture were calculated by Rietveld refinement and estimated to be 46.43% and 53.56%, respectively. EuH_9 was found to be isostructural to the earlier synthesized ThH_9 [16], YH_9 [20,21], CeH_9 [14,15], NdH_9 [18], and PrH_9 [27] [Fig. 2(d)], in which each metal atom is surrounded by 29 H atoms forming a H_{29} cage and each cage is composed of six irregular squares, six pentagons, and six hexagons. We note this phase has been reproduced by another work after we reported it in the initial version [56]. It should be noted that there are still some unidentified XRD patterns marked by asterisks, which may be related to the unexpected Eu_xH_y compounds due to the temperature and pressure gradients in the laser-heated diamond-anvil cell experiments. In this research, we have carried out Raman measurements on the synthesized EuH_x, but a Raman signal only for diamond and hydrogen could be detected.

The existence of f electrons in lanthanide (except La) usually leads to the appearance of magnetism in the hydrides [18,27]. *Ab initio* calculations predicted that all neodymium superhydrides in Ref. [18] have antiferromagnetic order at high pressures. Given the local feature of seven f electrons for the Eu element even up to 119 GPa, we have performed spin-polarized calculations on our synthesized Eu-H system. In order to investigate the magnetic configurations of these structures, we built up a supercell of four metal Eu atoms (Fig. S2) except for EuH_5 by using the derivative structure enumeration library ENUMLIB [57], where all magnetic configurations were calculated with experimental lattice parameters. As a result, a strong magnetic moment was found in all the synthesized Eu-H compounds (Table S2) with $\sim 7\mu_B$ per Eu atom at a pressure range of 80–180 GPa (Fig. S3 [40]). Further simulations show the ferromagnetic feature of $Pm\bar{3}n$ EuH_5 and $Im\bar{3}m$ EuH_6, and the antiferromagnetic feature of $Fm\bar{3}m$ EuH_3, $P6_3/mmc$ EuH_6, and $P6_3/mmc$ EuH_9.

Furthermore, we fitted the EOS of all stoichiometries with the consideration of magnetism and spin-orbit coupling and compared with the experimental pressure-volume data [Fig. 3(b)]. It can be found that the experimental unit cell parameters and volumes are in good agreement with the theoretical data, which give further support to the validity of the structures and stoichiometries we identified from the XRD data.

To identify the bonding nature of hydrogen in clathrate superhydride, the electron localization function (ELF) was also calculated in EuH_6 and EuH_9 (Fig. S2 [40]). The weak electron localization (0.5–0.6) between H atoms indicates weak covalent bond characteristics and a three-dimensional network structure in the H cages. An analysis of the electronic band structure illustrates that all the stoichiometries synthesized in

this work present a metallic character at high pressures owing to the overlap of the conduction and valence bands at the Fermi level as shown in Figs. S4 and S5 [40].

Electrical resistance measurements as an efficient way to characterize the superconducting transition or magnetic order transition have been carried out using a four-probe technique for two samples after heating to about 1500 and 2000 K at 140 GPa, respectively, as shown in Fig. S7. The resistance decreases linearly during cooling at temperatures above 225 K in sample 1 and 258 K in sample 2, indicating their metallic nature. At lower temperatures, the slopes of the resistance-temperature (R-T) curves become larger, as indicated by the red lines, implying an increase of the rates of resistance drop, which, however, are still very slow compared with the typical superconducting transition where resistance normally drops to zero within 10 K. Interestingly, the profiles of the R-T curves are similar to the magnetic transition in lanthanide elements such as Eu [30] and Tb [58]. Referring to the synthesized conditions of different superhydrides in the above XRD measurements, we infer that the temperatures of 225 and 258 K at the kink points may indicate the Curie temperature of $Pm\bar{3}n$ EuH_5 and $Im\bar{3}m$ EuH_6, respectively. A detailed study of the magnetic order transition in the Eu-H system is beyond the scope of this paper, but the current work may shed light on future experiments on magnetic superhydrides.

IV. CONCLUSION

In summary, we have successfully synthesized a series of europium superhydrides, including EuH_3, EuH_5, EuH_6, and EuH_9, in the pressure range of 80–170 GPa. Among these hydrides, EuH_6 and EuH_9 have clathrate structures with an atomiclike hydrogen sublattice surrounding Eu atoms. Two nonclathrate structured phases of EuH_5 and EuH_6 are reported here for the prototype structure models in a system of lanthanide superhydrides. The calculation results show that all europium hydrides exhibit strong magnetism at the pressure range considered in the present study. This work paves the way for further experimental investigations on the complex mechanism of magnetism, the strongly correlated effect, and superconductivity on Eu superhydrides.

ACKNOWLEDGMENTS

This work was supported by the Major Program of the National Natural Science Foundation of China (Grant No. 52090024), Strategic Priority Research Program of Chinese Academy of Sciences (Grant No. XDB33000000), National Key R&D Program of China (Grant No. 2018YFA0305900), National Natural Science Foundation of China (Grants No. 11874175, No. 12074139, No. 12074138, No. 11874176, No. 12034009, and No. 11974134), Jilin Province Outstanding Young Talents Project (Grant No. 20190103040JH), and Program for JLU Science and Technology Innovative Research Team (JLUSTIRT). We used the computing facilities at the High-Performance Computing Centre of Jilin University and Tianhe2-JK at the Beijing Computational Science Research Centre. XRD measurement were performed at BL10XU/SPring-8, Shanghai Synchrotron Radiation Facility Beamline BL15U1 and Beijing Synchrotron Radiation Facility HP-Station 4W2.

The authors declare no competing interests.

[1] N. W. Ashcroft, Metallic Hydrogen: A High-Temperature Superconductor? Phys. Rev. Lett. **21**, 1748 (1968).

[2] P. Loubeyre, F. Occelli, and P. Dumas, Synchrotron infrared spectroscopic evidence of the probable transition to metal hydrogen, Nature (London) **577**, 631 (2020).

[3] M. I. Eremets, A. P. Drozdov, P. P. Kong, and H. Wang, Semimetallic molecular hydrogen at pressure above 350 GPa, Nat. Phys. **15**, 1246 (2019).

[4] P. Dalladay-Simpson, R. T. Howie, and E. Gregoryanz, Evidence for a new phase of dense hydrogen above 325 gigapascals, Nature (London) **529**, 63 (2016).

[5] H. Wang, J. S. Tse, K. Tanaka, T. Iitaka, and Y. Ma, Superconductive sodalite-like clathrate calcium hydride at high pressures, Proc. Natl. Acad. Sci. USA **109**, 6463 (2012).

[6] H. W. Kroto, J. R. Heath, S. C. O'Brien, R. F. Curl, and R. E. Smalley, C_{60}: buckminsterfullerene, Nature (London) **318**, 162 (1985).

[7] J. S. Kasper, P. Hagenmuller, M. Pouchard, and C. Cros, Clathrate structure of silicon Na_8Si_{46} and Na_xSi_{136} ($x < 11$), Science **150**, 1713 (1965).

[8] Y. Li, J. Hao, H. Liu, J. S. Tse, Y. Wang, and Y. Ma, Pressure-stabilized superconductive yttrium hydrides, Sci. Rep. **5**, 9948 (2015).

[9] X. Feng, J. Zhang, G. Gao, H. Liu, and H. Wang, Compressed sodalite-like MgH_6 as a potential high-temperature superconductor, RSC Adv. **5**, 59292 (2015).

[10] F. Peng, Y. Sun, C. J. Pickard, R. J. Needs, Q. Wu, and Y. Ma, Hydrogen Clathrate Structures in Rare Earth Hydrides at High Pressures: Possible Route to Room-Temperature Superconductivity, Phys. Rev. Lett. **119**, 107001 (2017).

[11] H. Liu, I. I. Naumov, R. Hoffmann, N. W. Ashcroft, and R. J. Hemley, Potential high-T_c superconducting lanthanum and yttrium hydrides at high pressure, Proc. Natl. Acad. Sci. USA **114**, 6990 (2017).

[12] M. Somayazulu, M. Ahart, A. K. Mishra, Z. M. Geballe, M. Baldini, Y. Meng, V. V. Struzhkin, and R. J. Hemley, Evidence for Superconductivity above 260 K in Lanthanum Superhydride at Megabar Pressures, Phys. Rev. Lett. **122**, 027001 (2019).

[13] A. P. Drozdov, P. Kong, V. S. Minkov, S. P. Besedin, M. A. Kuzovnikov, S. Mozaffari, L. Balicas, F. F. Balakirev, D. E. Graf, V. B. Prakapenka *et al.*, Superconductivity at 250 K in lanthanum hydride under high pressures, Nature (London) **569**, 528 (2019).

[14] X. Li, X. Huang, D. Duan, C. J. Pickard, D. Zhou, H. Xie, Q. Zhang, Y. Huang, Q. Zhou, B. Liu *et al.*, Polyhydride CeH_9 with an atomic-like hydrogen clathrate structure, Nat. Commun. **10**, 3461 (2019).

[15] N. P. Salke, M. M. Esfahani, Y. Zhang, I. A. Kruglov, J. Zhou, Y. Wang, E. Greenberg, V. B. Prakapenka, J. Liu, A. R. Oganov *et al.*, Synthesis of clathrate cerium superhydride CeH_9 at 80–100 GPa with atomic hydrogen sublattice, Nat. Commun. **10**, 4453 (2019).

[16] D. V. Semenok, A. G. Kvashnin, A. G. Ivanova, V. Svitlyk, V. Y. Fominski, A. V. Sadakov, O. A. Sobolevskiy, V. M. Pudalov, I. A. Troyan, and A. R. Oganov, Superconductivity at 161 K in thorium hydride ThH_{10}: Synthesis and properties, Mater. Today **33**, 36 (2020).

[17] T. Matsuoka, M. Hishida, K. Kuno, N. Hirao, Y. Ohishi, S. Sasaki, K. Takahama, and K. Shimizu, Superconductivity of platinum hydride, Phys. Rev. B **99**, 144511 (2019).

[18] D. Zhou, D. V. Semenok, H. Xie, X. Huang, D. Duan, A. Aperis, P. M. Oppeneer, M. Galasso, A. I. Kartsev, A. G. Kvashnin *et al.*, High-pressure synthesis of magnetic neodymium polyhydrides, J. Am. Chem. Soc. **142**, 2803 (2020).

[19] I. A. Troyan, D. V. Semenok, A. G. Kvashnin, A. V. Sadakov, O. A. Sobolevskiy, V. M. Pudalov, A. G. Ivanova, V. B. Prakapenka, E. Greenberg, A. G. Gavriliuk *et al.*, Anomalous high-temperature superconductivity in YH_6, Adv. Mater. **33**, 2006832 (2021).

[20] E. Snider, N. Dasenbrock-Gammon, R. McBride, X. Wang, N. Meyers, K. V. Lawler, E. Zurek, A. Salamat, and R. P. Dias, Synthesis of Yttrium Superhydride Superconductor with a Transition Temperature up to 262 K by Catalytic Hydrogenation at High Pressures, Phys. Rev. Lett. **126**, 117003 (2021).

[21] P. Kong, V. S. Minkov, M. A. Kuzovnikov, A. P. Drozdov, S. P. Besedin, S. Mozaffari, L. Balicas, F. F. Balakirev, V. B. Prakapenka, S. Chariton *et al.*, Superconductivity up to 243 K in the yttrium-hydrogen system under high pressure, Nat. Commun. **12**, 5075 (2021).

[22] D. V. Semenok, I. A. Troyan, A. G. Ivanova, A. G. Kvashnin, I. A. Kruglov, M. Hanfland, A. V. Sadakov, O. A. Sobolevskiy, K. S. Pervakov, I. S. Lyubutin *et al.*, Superconductivity at 253 K in lanthanum-yttrium ternary hydrides, Materials Today **48**, 18 (2021).

[23] W. Chen, D. V. Semenok, A. G. Kvashnin, X. Huang, I. A. Kruglov, M. Galasso, H. Song, D. Duan, A. F. Goncharov, V. B. Prakapenka *et al.*, Synthesis of molecular metallic barium superhydride: pseudocubic BaH_{12}, Nat. Commun. **12**, 273 (2021).

[24] L. Ma, K. Wang, Y. Xie, X. Yang, Y. Wang, M. Zhou, H. Liu, X. Yu, Y. Zhao, H. Wang *et al.*, Experimental observation of superconductivity at 215 K in calcium superhydride under high pressures, arXiv:2103.16282.

[25] Z. W. Li, X. He, C. L. Zhang, S. J. Zhang, S. M. Feng, X. C. Wang, R. C. Yu, and C. Q. Jin, Superconductivity above 200 K observed in superhydrides of calcium, arXiv:2103.16917.

[26] W. Chen, D. V. Semenok, X. Huang, H. Shu, X. Li, D. Duan, T. Cui, and A. R. Oganov, High-Temperature Superconducting Phases in Cerium Superhydride with a T_c up to 115 K below a Pressure of 1 Megabar, Phys. Rev. Lett. **127**, 117001 (2021).

[27] D. Zhou, D. V. Semenok, D. Duan, H. Xie, W. Chen, X. Huang, X. Li, B. Liu, A. R. Oganov, and T. Cui, Superconducting praseodymium superhydrides, Sci. Adv. **6**, eaax6849 (2020).

[28] J. C. Bunzli, Europium in the limelight, Nat. Chem. **2**, 696 (2010).

[29] T. Wang, D. Zhao, X. Guo, J. Correa, B. L. Riehl, and W. R. Heineman, Carbon nanotube-loaded Nafion film electrochemical sensor for metal ions: Europium, Anal. Chem. **86**, 4354 (2014).

[30] M. Debessai, T. Matsuoka, J. J. Hamlin, J. S. Schilling, and K. Shimizu, Pressure-Induced Superconducting State of Europium Metal at Low Temperatures, Phys. Rev. Lett. **102**, 197002 (2009).

[31] B. Johansson and A. Rosengren, Generalized phase diagram for the rare-earth elements: Calculations and correlations of bulk properties, Phys. Rev. B **11**, 2836 (1975).

[32] A. Rosengren and B. Johansson, Alloy theory of the intermediate valence state: Application to europium metal, Phys. Rev. B **13**, 1468 (1976).

[33] W. Bi, J. Lim, G. Fabbris, J. Zhao, D. Haskel, E. E. Alp, M. Y. Hu, P. Chow, Y. Xiao, W. Xu *et al.*, Magnetism of europium under extreme pressures, Phys. Rev. B **93**, 184424 (2016).

[34] H. Saitoh, A. Machida, T. Matsuoka, and K. Aoki, Phase diagram of the Eu-H system at high temperatures and high hydrogen pressures, Solid State Commun. **205**, 24 (2015).

[35] T. Matsuoka *et al.*, Structural and Valence Changes of Europium Hydride Induced by Application of High-Pressure H_2, Phys. Rev. Lett. **107**, 025501 (2011).

[36] Y. Akahama and H. Kawamura, Pressure calibration of diamond anvil Raman gauge to 310 GPa, J. Appl. Phys. **100**, 043516 (2006).

[37] N. Hirao, S. I. Kawaguchi, K. Hirose, K. Shimizu, E. Ohtani, and Y. Ohishi, New developments in high-pressure X-ray diffraction beamline for diamond anvil cell at SPring-8, Matter Radiat. Extremes. **5**, 018403 (2020).

[38] C. Prescher and V. B. Prakapenka, DIOPTAS: a program for reduction of two-dimensional X-ray diffraction data and data exploration, High Pressure Res. **35**, 223 (2015).

[39] B. H. Toby, EXPGUI, a graphical user interface for GSAS, J. Appl. Crystallogr. **34**, 210 (2001).

[40] See Supplemental Material at http://link.aps.org/supplemental/10.1103/PhysRevResearch.3.043107 for full lists of detailed crystal information, magnetic configurations, and calculated electronic band and electrical resistance measurements.

[41] P. Hohenberg and W. Kohn, Inhomogeneous electron gas, Phys. Rev. **136**, B864 (1964).

[42] W. Kohn and L. J. Sham, Self-consistent equations including exchange and correlation effects, Phys. Rev. **140**, A1133 (1965).

[43] J. P. Perdew, K. Burke, and M. Ernzerhof, Generalized Gradient Approximation Made Simple, Phys. Rev. Lett. **77**, 3865 (1996).

[44] P. E. Blöchl, Projector augmented-wave method, Phys. Rev. B **50**, 17953 (1994).

[45] G. Kresse and D. Joubert, From ultrasoft pseudopotentials to the projector augmented-wave method, Phys. Rev. B **59**, 1758 (1999).

[46] G. Kresse and J. Hafner, *Ab initio* molecular dynamics for open-shell transition metals, Phys. Rev. B **48**, 13115 (1993).

[47] G. Kresse and J. Hafner, *Ab initio* molecular-dynamics simulation of the liquid-metal-amorphous-semiconductor transition in germanium, Phys. Rev. B **49**, 14251 (1994).

[48] G. Kresse and J. Furthmiller, Efficiency of ab-initio total energy calculations for metals and semiconductors using a plane-wave basis set, Comput. Mater. Sci. **6**, 15 (1996).

[49] R. J. Husband, I. Loa, G. W. Stinton, S. R. Evans, G. J. Ackland, and M. I. McMahon, Europium-IV: An Incommensurately Modulated Crystal Structure in the Lanthanides, Phys. Rev. Lett. **109**, 095503 (2012).

[50] F. Birch, Finite elastic strain of cubic crystals, Phys. Rev. **71**, 809 (1947).

[51] A. J. Maeland and D. E. Holmes, Inelastic neutron scattering spectra from lanthanum dihydride and lanthanum trihydride, J. Chem. Phys. **54**, 3979 (1971).

[52] R. E. Rundle, The hydrogen positions in uranium hydride by neutron diffraction, J. Am. Chem. Soc. **73**, 4172 (1951).

[53] Y. Wang, J. Lv, L. Zhu, and Y. Ma, CALYPSO: A method for crystal structure prediction, Comput. Phys. Commun. **183**, 2063 (2012).

[54] Y. Wang, J. Lv, L. Zhu, and Y. Ma, Crystal structure prediction via particle-swarm optimization, Phys. Rev. B **82**, 094116 (2010).

[55] S. Qian, X. Sheng, X. Yan, Y. Chen, and B. Song, Theoretical study of stability and superconductivity of ScH_n ($n = 4$–8) at high pressure, Phys. Rev. B **96**, 094513 (2017).

[56] D. V. Semenok, D. Zhou, A. G. Kvashnin, X. Huang, M. Galasso, I. A. Kruglov, A. G. Ivanova, A. G. Gavriliuk, W. Chen, N. V. Tkachenko *et al.*, Novel strongly correlated europium superhydrides, J. Phys. Chem. Lett. **12**, 32 (2020).

[57] G. L. W. Hart, L. J. Nelson, and R. W. Forcade, Generating derivative structures at a fixed concentration, Comput. Mater. Sci. **59**, 101 (2012).

[58] J. Lim, G. Fabbris, D. Haskel, and J. S. Schilling, Anomalous pressure dependence of magnetic ordering temperature in Tb revealed by resistivity measurements to 141 GPa: Comparison with Gd and Dy, Phys. Rev. B **91**, 174428 (2015).